ELSEVIER

Sedimentary Geology 134 (2000) 129–147

Sedimentary Geology

www.elsevier.nl/locate/sedgeo

Sequence-stratigraphic significance of Miocene to Pliocene glauconite-rich layers, on- and offshore of the US Mid-Atlantic margin

L.C. Harris, B.M. Whiting*

Geology Department, Central Washington University, Ellensburg, WA 98926, USA

Abstract

Glauconite is generally agreed to be a reliable indicator of low sedimentation rate, but little systematic work has been done to specify the role of glauconite in a sequence-stratigraphic framework. Ocean Drilling Program Leg 174A recovered a good record of late Tertiary sediments along the shelf edge of the New Jersey US Atlantic margin, and glauconite was present in many intervals of the cores, sometimes in vertical proximity to sequence boundaries. Leg 174A glauconite was analyzed with binocular microscope, XRD and SEM to determine the percent of potassium and degree of maturity in order to relate occurrence to depositional environment. Seismic data were used to locate sequence boundaries, and percent glauconite was visually estimated. Glauconite samples from Site 1073 were found to have formed within a lowstand systems tract (LST), and as part of a distal condensed section (CS) within a transgressive systems tract (TST). These results are comparable to those from nearby Site 903 of Leg 150, which indicate a similar depositional setting for glauconite. Glauconites at shelf Sites 1071 and 1072 likely formed in the TST as well. Onshore, glauconite occurs mainly in transgressive systems tracts. The Miocene appears to be the upper limit of glauconite formation onshore. As the magnitude of sea-level change decreased, present onshore locations became too nearshore to maintain sediment-free environments, and the zone of glauconite deposition moved seaward. The same process did not occur offshore until the Plio–Pleistocene. Low subsidence-rate margins such as the US Atlantic are subject more to the variations of sea-level than to changes in sediment supply, tectonics, or other factors influencing their depositional patterns. Although glauconite occurrence is widespread in the stratigraphic record, this study demonstrates that for low subsidence-rate margins, primary deposition of glauconite is largely restricted to the TST.

Keywords: sequence stratigraphy; glauconite; US Atlantic margin; continental shelf; continental slope

1. Introduction

The exact sequence-stratigraphic significance of glauconite has long been problematic, in part because a wide variety of depositional settings has been proposed (Table 1). Deposition of glauconite is typically inferred to represent slow rates of clastic influx and is most commonly associated with development of condensed sections (Baum and Vail, 1988; Loutit et al., 1988; Amorosi, 1995). However, there are many depositional settings in which glauconite will form, such as maximum flooding surfaces, incised valley fill, shelf margin wedges, and proximal lowstand wedges (Table 1), and more work is needed to constrain its range of occurrence in the stratigraphic record. In a systems-tract context, glauconite is often inferred to be present at the base of the transgressive

* Corresponding author Fax: + 1-509-963-2821.
E-mail address: bmw@geology.cwu.edu (B.M. Whiting).

0037-0738/00/$ - see front matter
PII: S0037-0738(00)00017-8

Table 1
Possibilities for glauconite occurrence (after Amorosi, 1995)[a]

Sequence-stratigraphic setting	Glauconite maturity
Upper part of parasequence (HST)	Low to very high
Lower part of parasequence (HST)	Low to moderate
Maximum flooding surface (CS)	High to very high
Uppermost TST-lowermost HST (CS)	High to very high
Ravinement surface (TST)	Variable
Incised valley fill (TST)	Low to moderate
Upper part of parasequence (TST)	Low to moderate
Lower part of parasequence (TST)	Low to high
Shelf margin wedge (LST)	Low to moderate
Proximal lowstand wedge (LST)	Variable
Lowstand fan complex (LST)	Variable

[a] HST = Highstand System Tract; CS = Condensed Section; TST = Transgressive System Tract; and LST = Lowstand System Tract.

systems tract (TST) and in the entire TST marking the base of each component parasequence (Amorosi, 1995; Table 1).

The exact chemical mode of glauconite formation is not well understood. Am Ende (1995) expanded on the work of Manheim (1967) by proposing that during lowstand, aquifers that are recharged on the shelf and discharge on the slope have a higher hydraulic head, and thus may provide a source of iron-rich groundwater needed to mix with potassium in seawater to form glauconite at the discharge point. This mechanism was proposed as a way to circumvent the fact that seawater is not rich in Fe, and as an explanation for the limited extent of glauconite deposits. However, this mechanism requires connectivity of aquifers that is difficult to resolve with seismic or drilling data.

An objective of both Ocean Drilling Program (ODP) Legs 150 and 174A was to further constrain the sequence-stratigraphic setting and sedimentary history of the Atlantic margin (Mountain et al., 1994; Austin et al., 1998). Glauconite is important in this analysis because of its autochthonous nature, as it can provide important clues to the sedimentary environment during its formation. Glauconite has several stages of developmental maturity (Table 1) and may require 10^5–10^6 years to form (Odin and Matter, 1981). Therefore, the developmental stage of glauconite may indicate conditions during its growth. McCracken et al. (1994) focused on six glauconite deposits from Site 903 of Leg 150 and analyzed the sedimentologic, petrologic, and geochemical nature of the layers. They evaluated the in situ versus transported nature of glauconite, amounts of terrigenous versus biogenic material, and the sedimentologic and diagenetic features of the lower boundaries of the units. Site 903 has some characteristics in common with Leg 174A Site 1073: both sites are located just off the shelf (Fig. 1), approximately 56 km apart, and the water depth for both is similar (Site 903 had a water depth of approximately 443 m, and Site 1073 had a water depth of 639.4 m). Comparisons between Sites 1073 and 903 are facilitated by the excellent (~100%) core recovery at both locations.

The objectives of this study include: (1) an initial determination of the sequence-stratigraphic significance of glauconite at Sites 1071, 1072 and 1073; (2) comparison of those results with conclusions from Site 903; (3) integration with other Leg 174A results; (4) an interpretation of the sequence-stratigraphic significance of glauconite relative to classic Exxon geometric models (e.g. Posamentier et al., 1988) and to the proposed Leg 174A systems-tract geometry of Christie-Blick and Austin (1998); Fig. 2); and (5) correlation of offshore with onshore glauconite occurrence. While it is likely that there is no one single sequence-stratigraphic mode of occurrence of glauconite that applies to all margins, data and samples from Legs 174A and 150 and onshore Legs 174AX and 150X enable us to constrain glauconite occurrence in a fairly well-understood setting and, possibly, to eliminate some of the competing hypotheses for the sequence-stratigraphic significance of glauconite.

2. Geologic and sequence-stratigraphic setting

The US Atlantic margin is a type example of a mature passive margin, and thus has been relatively well studied. Rifting of North America began during the early Mesozoic, and formation of the central Atlantic began during middle Mesozoic time (Hynes, 1990). Because rifting occurred so long ago, the crust has cooled at the present time to close to equilibrium (Steckler et al., 1988). Therefore, thermal and tectonic subsidence rates are extremely low. For example, Greenlee et al. (1988) determined a thermotectonic subsidence rate for the Tertiary of 6.5 m/m.y., and Steckler et al. (1988) calculated a Neogene rate of

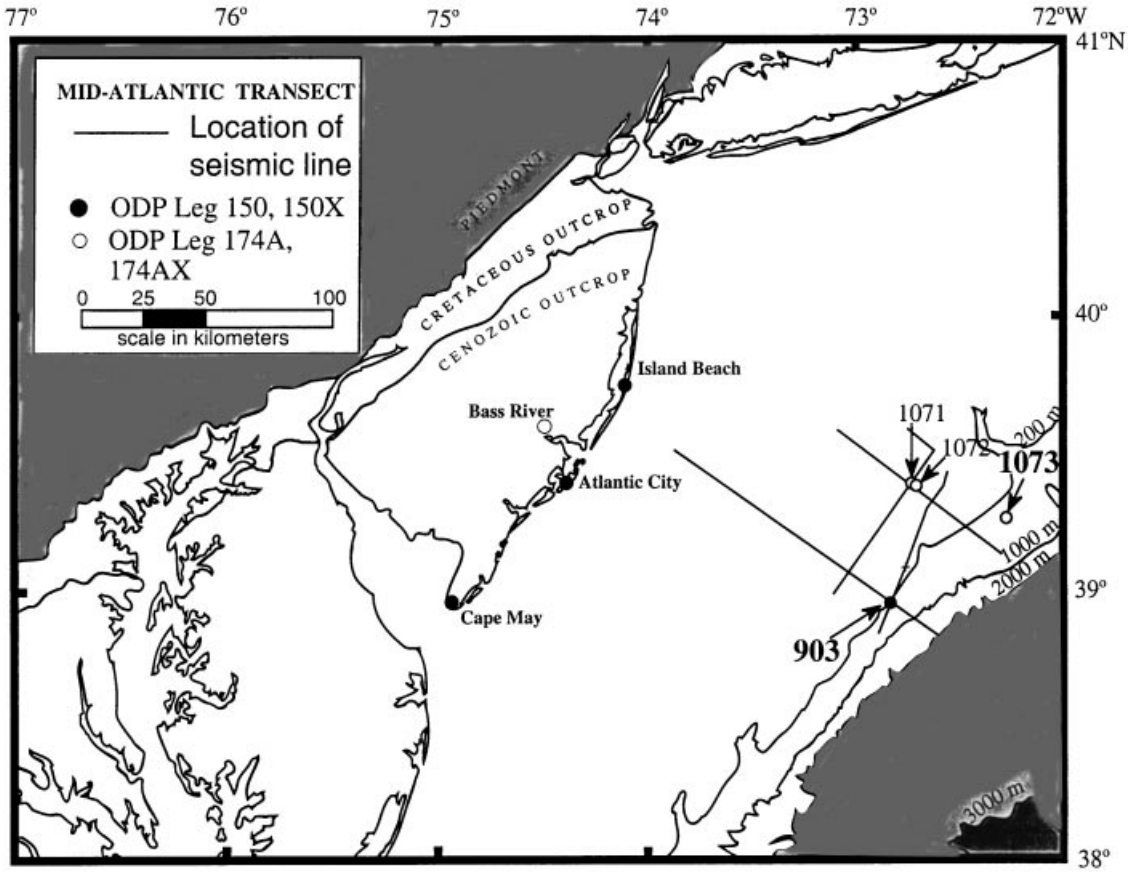

Fig. 1. Location map showing ODP Legs 150, 174A, 150X, and 174AX drilling sites and location of seismic lines. Note location of Sites 903 and 1073. Modified from Austin et al. (1998).

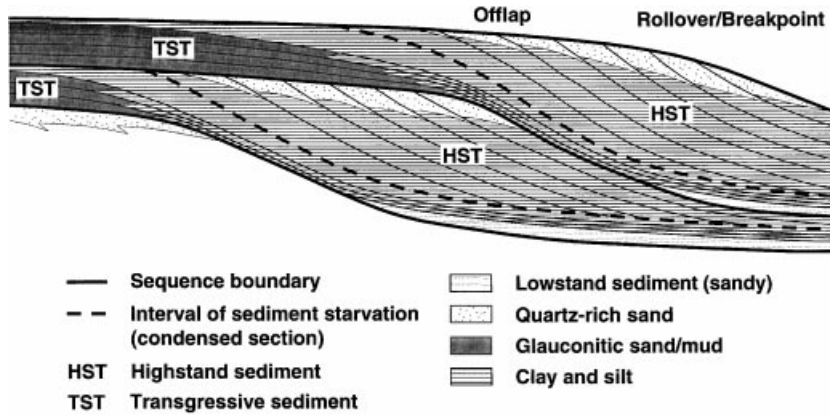

Fig. 2. Sequence stratigraphic model for New Jersey outer shelf. This diagram shows the proposed variations from the Exxon model, but not how these sequence boundaries would extend onto the slope where Sites 903 and 1073 are located (modified from Christie-Blick, pers. comm., and representing one model discussed in Austin et al., 1998). Deviations from the Exxon model are mainly the very thin LST, and the prograding clinoforms rather than aggradation in the HST.

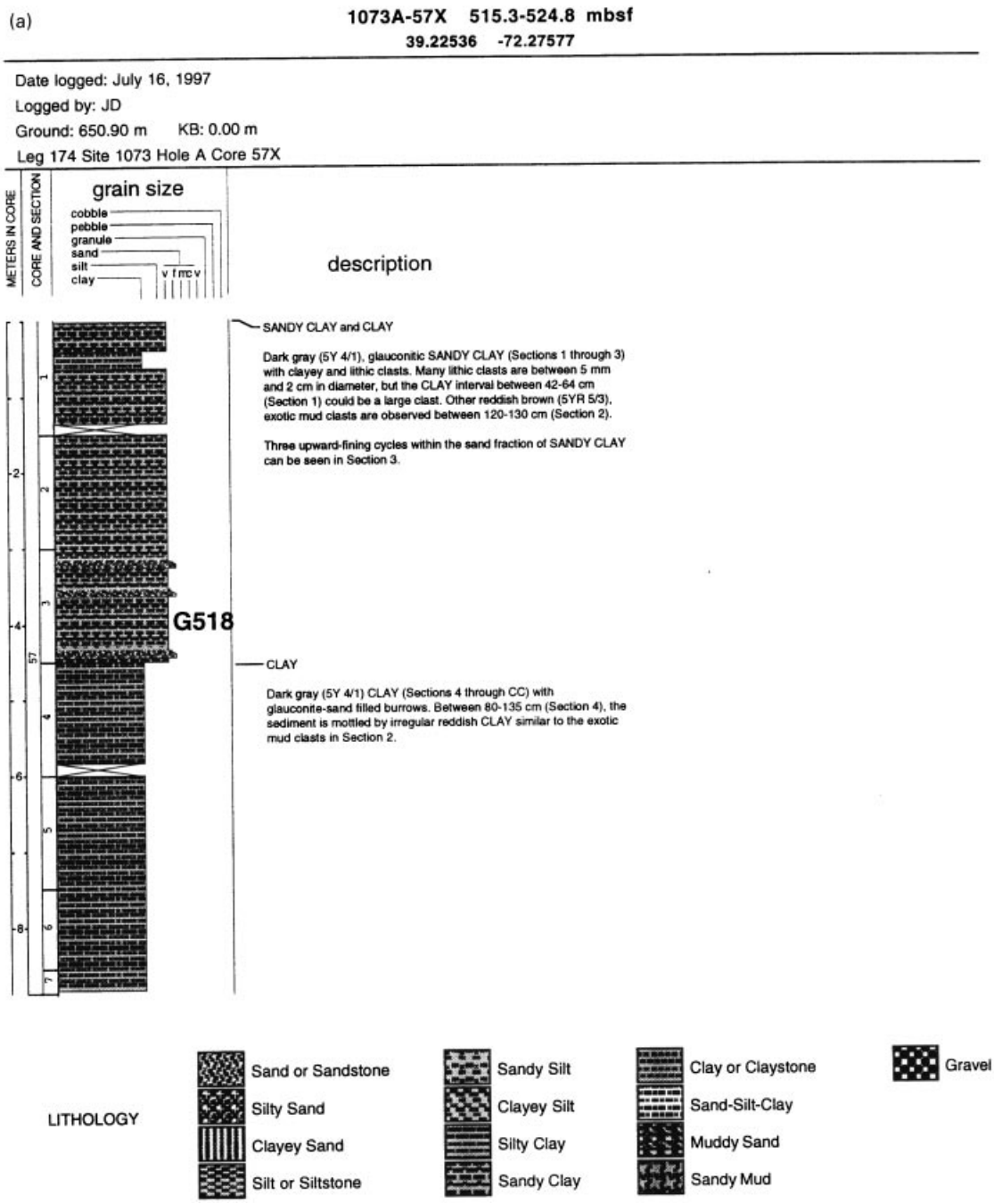

Fig. 3. Detailed sedimentologic logs from Site 1073: (a) core 1073A 57X; (b) 1073A 60X; and (c) 1073A 68X, showing grain sizes and a description of the core sample (from Austin et al., 1998).

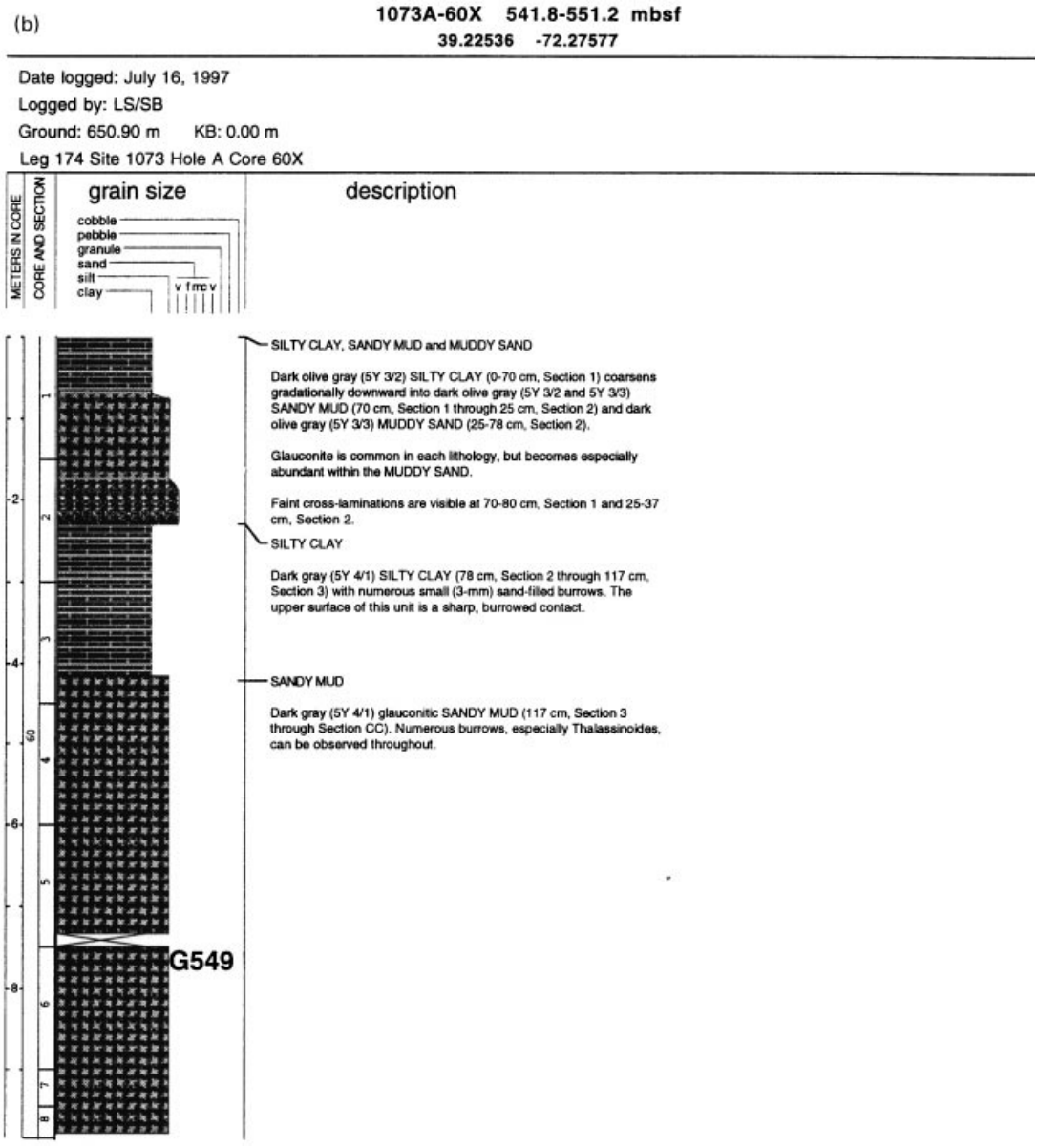

Fig. 3. (*continued*)

8 m/m.y. Thus, thermal subsidence is a relatively minor factor on the Atlantic margin, so accommodation is created primarily by eustatic sea-level variation, compaction, and by slumping on the slope.

Well-known glauconite occurrence and fairly well understood stratigraphy of the US Atlantic margin make on- and offshore New Jersey a good prospective location to constrain the sequence-stratigraphic occurrence of glauconite. Numerous sequence-stratigraphic studies have focused on the US Mid-Atlantic margin (Fig. 1) because of its lack of structural overprint, well-understood sediment supply, and availability of data. A recent study using seismic and well data

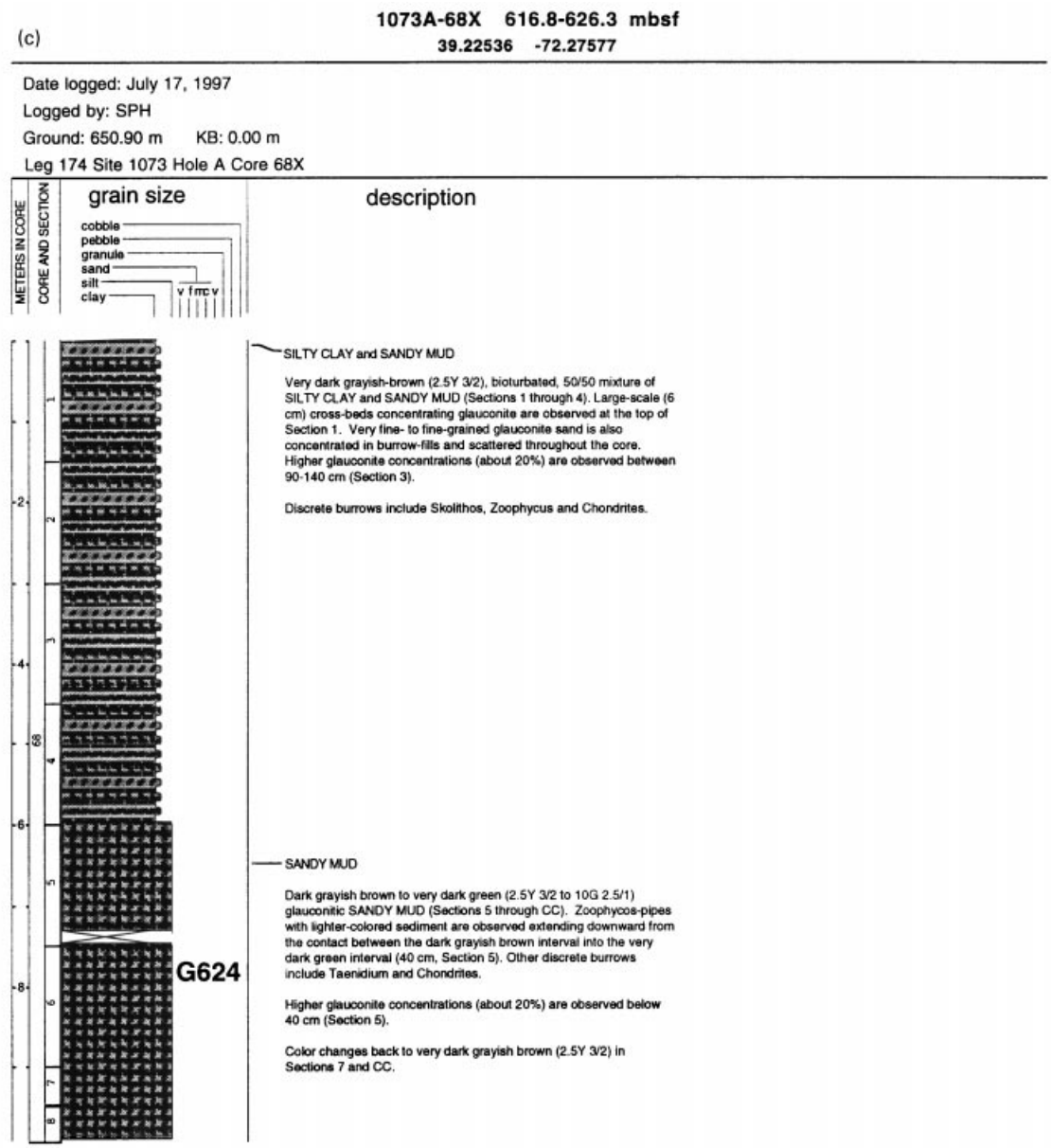

Fig. 3. (*continued*)

(Greenlee et al., 1992) reported a lack of TST on the Mid-Atlantic margin due to the low subsidence rate and lack of accommodation. In contrast preliminary results from Ocean Drilling Program Leg 174A sites indicate a lack of, or very thin, lowstand systems tracts (LST). This is possibly due to specifies of site locations on the shelf and upper slope off the New Jersey margin, and thick glauconite sand interpreted to be TST (Fig. 2; and Christie-Blick and Austin, 1998).

While it is agreed that eustasy is the driving force behind late Neogene sequence generation along this margin, and is itself likely driven by the changing size of continental ice sheets (Miller et al., 1998a), the

genetic significance of systems tract geometry at low-subsidence-rate margins remains controversial. The general lack of accommodation introduces some complications into the traditional Exxon model geometry of the Atlantic margin (e.g., Christie-Blick, 1990; Austin et al., 1998). For example, preliminary Leg 174A results showed that no shelfal LST is present off the New Jersey margin (Austin et al., 1998). Furthermore, preliminary leg results (Austin et al., 1998) imply that the signature of the HST is early progradation with little vertical aggradation; progradation takes place later in the Exxon model (Posamentier et al., 1988). The low subsidence rate of the Atlantic margin leaves little space to be filled, so the time period over which aggradation is possible is much shorter compared to higher subsidence margins. If this is the case, condensed sections have a shorter time interval in which to develop before being buried by prograding clinoforms. Thus, there is a shorter potential time interval for glauconite to form before being overwhelmed by sedimentation and potentially reworked.

3. Data and methods

The data for this project is based on core samples collected from Leg 174A Sites 1071, 1072, and 1073 (Figs. 1 and 3), and shipboard measurements (Austin et al., 1998). Procedures used for glauconite analysis follow am Ende (1995) and Odin and Matter (1981). After initial hand-picking of samples with a binocular microscope, the presence of glauconite was confirmed through X-ray diffraction, which also allowed determination of potassium content (discussed below). Glauconite grains (Fig. 4) were powdered and analyzed with XRD on a low-background sample holder.

Odin and Matter (1981) recognized four stages of maturity of glauconite: nascent, slightly evolved, evolved, and highly evolved. Maturity can also be referred to as the degree of glauconitization or verdissement. Nascent grains are light green in color and are likely to retain the shape of the test or grain that is being replaced. Slightly evolved grains are green in color and show the beginnings of cracks from the growth of the glauconite minerals inside the grain. Evolved grains have distinct cracks and are a darker green. Highly evolved grains are smooth, very dark green, and in some cases may even appear black (Odin and Matter, 1981; Odin and Fullagar, 1988; am Ende, 1995). Stage of maturity is one of the determining factors in narrowing the environment of formation; the longer the location remained free of detrital influx, the more mature the grains may become. The maturity of the glauconite grain was estimated through examination by binocular and scanning electron microscopes (Fig. 4). Color and morphology were the dominant factors used in the determination of maturity, following Odin and Matter (1981). Potassium oxide percent was estimated with the XRD data, following the procedure outlined by Odin and Fullagar (1988); more mature glauconite grains have a higher potassium oxide percentage. Using the XRD procedure to determine the potassium content quantifies the glauconite maturity better than relying solely on a visual estimate. However, the XRD procedure can be in error because of the possible presence of other clays and any coatings that remain in the sample. A peak created by an unknown component could be mistaken for that of glauconite, and used in the calculation if it is near the (020) peak at $19.6°2\theta$, or the (001) peak at $8.87°2\theta$. Both methods appear to be reliable, however, as the results of both generally agreed (Table 2).

4. Results from Leg 174A

Glauconite from Sites 1071 and 1072, and three main glauconite layers from Site 1073 were the focus of this study (Figs. 1 and 3). The glauconites from Site 1073 were located at 518 m below sea floor (mbsf), at 549 mbsf, and at 624 mbsf, and will be referred to as G_{518}, G_{549}, and G_{624}, respectively.

4.1. Site 1073

As previously discussed, color, morphology, and potassium percent of the glauconites (Table 2) were the basis for determining the maturity of the grains. G_{518} (Fig. 4c) is visually interpreted to be a highly evolved glauconite, yet it only contains approximately 7% K, which is consistent with evolved glauconite (Table 2a, Fig. 5a). This result varies from the visual estimation of the morphology because the XRD gives a result for all the powder on the sample holder, which

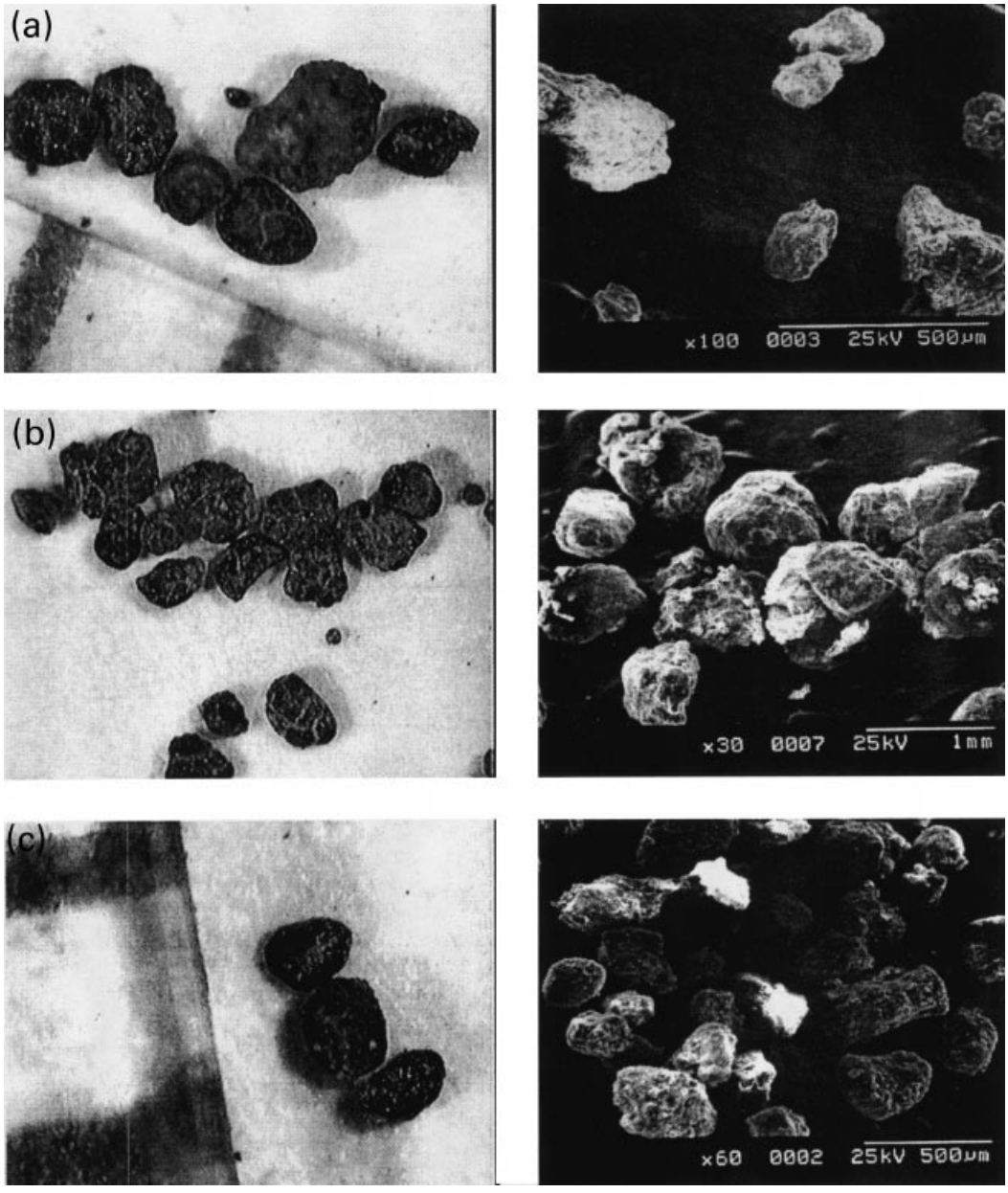

Fig. 4. Photomicrographs (left) and SEM photos (right) of 3 selected samples from Site 1073 showing typical grains from the different glauconite developmental stages. Marks on ruler indicate 1 mm each; field of view of other is 5 mm. (a) Sample 1073A 60X 2W 65.0–67.0, a slightly evolved to evolved sample, grains ranged from light green and very cracked to darker green and slightly cracked. (b) 1073A 71X 7W 6.0–8.0, an evolved sample, grains are dark green in color and show well-developed cracking. (c) Sample 1073A 57X 3W 124.0–126.0, referred to in the text as G_{518}, a highly evolved sample, grains are dark green and have a smooth texture.

Table 2
Selected samples from Leg 174A Site 1073A. Data shown includes stratigraphic position; color, shape, maturity, and potassium oxide content of the glauconite grains; sorting, size distribution, and per cent glauconite of the sample; and meters below sea floor. (v = very, dk = dark, lt = light, g = green, r = rounded, ev = evolved, sl = slightly, hi = highly)

Site	Hole	Core	Section	Cm	Color	Shape	Maturity	K_20 (%)	Sorting	Size dist.	% Glauc.	Mbsf
1073	A	57X	2W	107–109	Dark green	Rounded	hi ev		Poor	sandy clay w/clayey and lithic clasts	10–20 ?	516.8
1073	A	57X	3W	74–76	Dark green		Hi ev		3 upward-fining cycles	sandy clay w/clayey and lithic clasts	30 ?[a]	518.3
1073	A	57X	3W	100–102	Dark green	Rounded	Ev	6.5 ev	3 upward-fining cycles	Sandy clay w/clayey and lithic clasts	~50[a]	518.3
1073	A	57X	3W	124–126	Dark green	Well-rounded	hi ev	7 ev	3 upward-fining cycles	Sandy clay	~100[a]	518.3
					Sequence			Boundary	PP4(S)			519.8
1073	A	60X	2W	33–35	V.dk green	Rounded-w.r.	hi ev	7 ev	Cross-lams	Muddy sand	Almost all[a]	543.3
1073	A	60X	2W	65–67	Green to dk g	Well-rounded	Sl ev-ev	8 ev-hiev		Muddy sand	~80	543.3
1073	A	60X	3W	115–118	Green	Sub-r-rounded	Ev	7.9 ev	Numerous burrows	Silty clay	~80	544.8
1073	A	60X	4W	49–51	Green	Sub-r-rounded	Ev	~7.5 ev	Numerous burrows	Sandy mud	~50	546.3
1073	A	60X	4W	104–107	Dark green	Sub-r-rounded	ev	Too broad	Numerous burrows	Sandy mud	>50	546.3
1073	A	60X	5W	73–76	Darkish gr	Rounded-sub r	ev	8.7 hi ev	Numerous burrows	Sandy mud	80	547.8
1073	A	60X	6W	53–55	Dk g to brown	Rounded	ev-hi ev	6.4 ev	Numerous burrows	Sandy mud	>80	549.3
1073	A	60X	6W	67–70	Green	Sub-r-rounded	ev	~7.5 ev	Numerous burrows	Sandy mud	~80	549.3
1073	A	61X	2W	116–118	It g-dk g		Sl ev-hi ev	8.7 hi ev	Abundant burrows	Sandy mud	80–90	551.42
1073	A	61X	3W	30–33	It green	Rounded	Sl ev-ev	(8.8 hi ev	Abundant burrows	Silty clay	~50	552.92
					Sequence			Boundary	M4(S) AND M5(S) ?			569–616
1073	A	63X	3W	127–129	Green-dk g	Rounded	Sl ev-hi ev	5.4 sl ev	Common burrows	Silty clay		572.4
1073	A	66X	1W	13–15	V. dk green	Rounded	Hi ev	Too broad	Bioturbated	Silty clay and sandy mud	~50	597.8
1073	A	66X	5W	123–125	It green-greer	Rounded	Range		Bioturbated	Silty clay and sandy mud	30 ?	603.8
1073	A	67X	3W	130–132	Dark green	Very tiny	?	Too broad	Bioturbated	Silty clay and sandy mud	≥75	610.2
1073	A	67X	5W	124–126	Dark green	Subrounded	ev		Bioturbated	Silty clay and sandy mud	40–50	613.2
1073	A	67X	6W	79–81	It g-dk g	Rounded	Sl ev-hi ev	~6.6 ev	Bioturbated	Silty clay and sandy mud	60–70	614.7
1073	A	68X	1W	108–110	Green-dk g	Rounded	Sl ev-hi ev?		Bioturbated	Silty clay and sandy mud	30 ?	616.8
					Sequence			Boundary	M5.6(S)			~622
1073	A	68X	5W	75–77	V. dk green	Well-rounded			Burrows	Sandy mud	~50	622.8
1073	A	68X	6W	79–81	Dark green		ev	7 ev	Burrows	W/finer matl		624.3
1073	A	70X	6W	96–98	Dark green	Rounded	ev-hi ev	~7.2 ev	Bioturbated	Silty clay and sandy mud	~50	643.3
1073	A	71X	1W	119–121	Dark green	Rounded	ev	(8.5 hi ev	Abundant burrows	Silty clay	~50	644.7
1073	A	71X	2W	50–52	Green	Rounded	Ev/hi ev	Too broad	Abundant burrows	Silty clay	50–70	646.2
1073	A	71X	3W	126–128	Dark green	Subrounded	ev	~7.8evhiev	Bioturbated	Silty clay and sandy mud	~50	647.7
1073	A	71X	5W	51–53	Green	Rounded-sub r	ev	6 sl ev-ev	Less distinct burrows	Sandy mud	~50	650.7
1073	A	71X	5W	121–123	Dark green	Rounded-sub r	ev-hi ev	7 ev	Less distinct burrows	Sandy mud	~50	650.7
1073	A	71X	7W	6.0–8.0	Dark green	Sub-rounded	ev	7 ev	Ill-defined burrows	Glauc is silt w/very fine sand	≥80	653.7

[a] Indicates possible transportation.

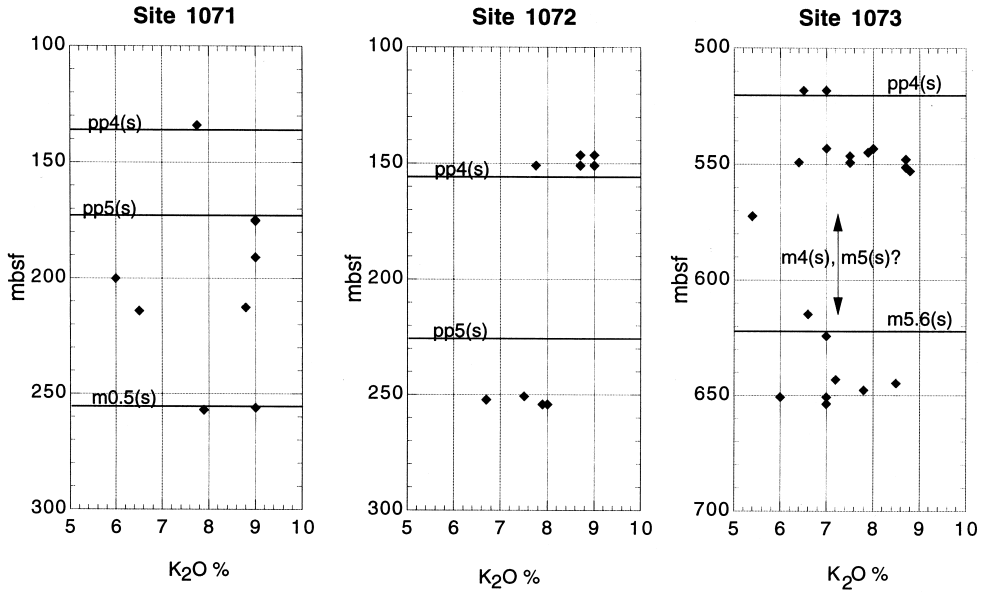

Fig. 5. Potassium percents of glauconite in comparison to meters below sea floor for Leg 174A Site 1073, Site 1072, and Site 1071. Sequence boundary locations from Austin et al. (1998); a range of possible locations is indicated when an exact position is unknown.

may have contained impurities that would skew the result, as discussed earlier. Fining-upward cycles in the G_{518} sediment (Table 2a) indicate possible transport of the glauconite, because graded bedding at this scale indicates a turbiditic deposition. Therefore, the glauconite may not have formed in this location or setting.

G_{549} is interpreted as evolved to highly evolved glauconite (6.4% K) (Table 2), and G_{624} is interpreted as an evolved glauconite deposit (7% K). Numerous burrows in both the G_{549} and G_{624} intervals suggest that the sediments at those depths were deposited without interference from transport. The portion of the section from which G_{549} was obtained showed an increase in the total γ-ray log and a large velocity contrast; G_{624} is also from an interval of increasing γ-ray values with an associated velocity contrast (Figs. 6 and 7).

At least two regionally correlatable sequence boundaries have been associated with Site 1073 (Austin et al., 1998; Mountain, pers. commun., 1998) (Fig. 7). The first is at ~79 mbsf and is immediately overlain by a distinct increase in the γ-ray log values (Figs. 6 and 7), but no glauconite is present at that depth (Fig. 4). The second sequence boundary is located at 520 mbsf (Fig. 7).

G_{518} shows evidence of being reworked. Grain size is sandy clay, and some clasts are present in the associated deposit (Fig. 3a); γ-ray values are low and indicate a fining upward trend (Fig. 6); the glauconite is highly evolved, and a sequence boundary is present immediately below the deposit. All of these factors suggest that G_{518} formed during lowstand. This description most closely resembles the G6 glauconite from Site 903 of McCracken et al. (1994; Fig. 6), which they describe as forming in place, but on a substrate of material eroded from updip and below the underlying sequence boundary and transported downdip during sea-level lowstand. The sequence boundary just below G_{518}, at 520 mbsf, is tentatively identified as pp4(s) (Fig. 7), which is uppermost Pliocene or lowermost Pleistocene in age (Austin et

Fig. 6. Comparison of Sites 903 and 1073 showing age, mbsf, sequence boundaries, lithology, glauconite occurrence, and γ-ray (from Austin et al., 1998, and after McCracken et al., 1994).

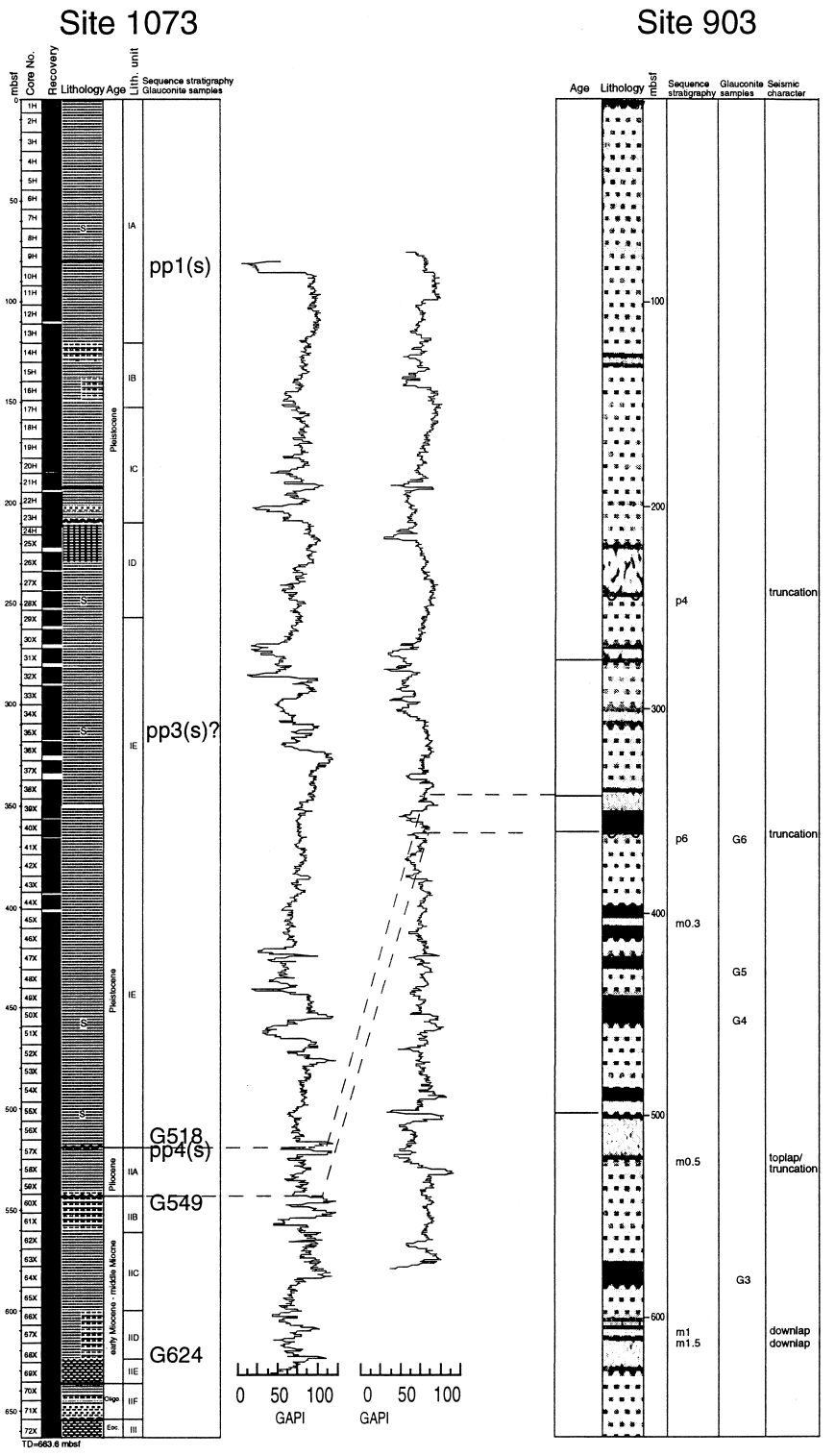
Site 1073
Site 903
mbsf
Core No.
Recovery
Lithology
Age
Lith. unit
Sequence stratigraphy
Glauconite samples
pp1(s)
pp3(s)?
G518
pp4(s)
G549
G624
Pleistocene
Pliocene
early Miocene - middle Miocene
Oligo
Eoc.
IA
IB
IC
ID
IE
IIA
IIB
IIC
IID
IIE
IIF
III
TD=663.6 mbsf
0 50 100
GAPI
0 50 100
GAPI
Age
Lithology
mbsf
Sequence stratigraphy
Glauconite samples
Seismic character
p4
p6
m0.3
m0.5
m1
m1.5
G6
G5
G4
G3
truncation
truncation
toplap/ truncation
downlap
downlap

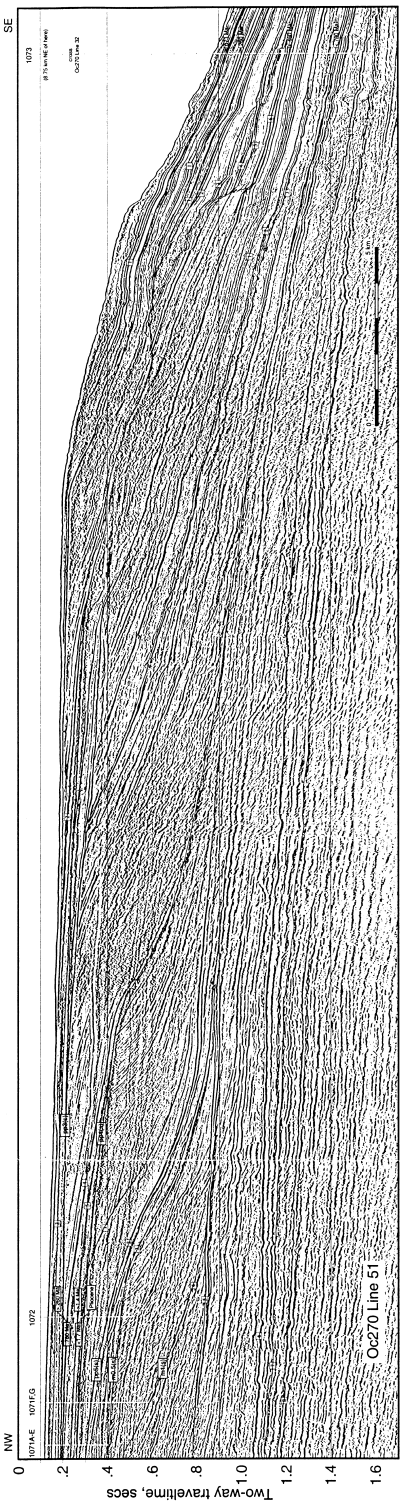

Fig. 7. Oceanus 270 Line 51 seismic data and preliminary interpretation (from G. Mountain, pers. commun.). Letters indicate reflectors that may be sequence boundaries but cannot be traced continuously.

al., 1998). This boundary correlates most closely to the p6 layer of McCracken et al. (1994) which is immediately overlain by their G6 deposit. However, biostratigraphy from Site 1073 indicates that pp4(s) and G_{518} are younger; therefore, an exact correlation between Sites 1073 and 903 is impossible. Both G6 and G_{518} are likely just above the base of Subunit IE (Fig. 6) above pp4(s).

G_{549} and G_{624} are interpreted as in situ deposits due to the presence of burrows throughout, the lack of clasts or other evidence of reworking (Fig. 3), and the evolved to highly evolved nature of the glauconite (Table 2). The γ-ray signature is high, and a reflector at approximately 596 mbsf (Fig. 7) marks a possible sequence boundary between the two deposits. However, this reflector cannot be confidently traced onto the shelf (Austin et al., 1998; Mountain, pers. comm., 1998). We interpret G_{549} and G_{624} to be distal condensed sections formed during transgression. McCracken et al. (1994) describe their G1 and G2 layers at Site 903 to have formed in the same setting (Fig. 6). G_{549} at Site 1073 is within lithostratigraphic unit IIB, perhaps upper Miocene in age (Figs. 3b and 6). This is approximately equivalent to lithostratigraphic unit III (Fig. 6) from Site 903 (Mountain et al., 1994).

4.2. Site 1072

At Site 1072, sequence boundary pp4(s) is located 141 and 155 mbsf (Table 3). Glauconites in this interval have potassium contents ranging from 7.75% (which indicates evolved) to >9% (highly evolved) (Fig. 5b). The poor sorting of the samples and subrounded shape indicate that the glauconite likely formed in place during the TST. This outer shelf location would have received little sediment input during both the lowstand and early transgression due to its interfluve location. The high potassium contents observed in the glauconites above the sequence boundary argue for a long time span with little sediment influx, which allowed maturation of the glauconite. According to Austin et al. (1998) and Christie-Blick et al. (1998) little to no deposition would have taken place at this location during the LST and TST due to the lack of accommodation space. Only during highstand are clinoforms created, at which time they prograde, building the margin outward. Therefore, highstand shedding would have prevented further glauconite maturation.

Glauconite between sequence boundaries pp5(s) and m0.5(s) (249–278 mbsf) ranges from 6.7–8% K (Fig. 5b), indicating mainly evolved glauconite. Poor sorting and subrounded shape indicate lack of significant transportation. If the glauconite has been transported, it will not yield useful information about the location at which it is found, since its environment of origin is elsewhere. This glauconite also likely formed during the TST, which provided adequate time for the verdissement process.

4.3. Site 1071

At Site 1071, glauconite between sequence boundaries pp5(s) and m0.5(s) are mostly highly evolved (Table 4, Fig. 5c). Core recovery was poor at Sites 1071 and 1072, so many sequence boundaries are not represented (Austin et al., 1998). However, it appears logical (based on comparison with Site 1072) that the glauconite with the highest potassium contents formed during the TST. The less mature glauconites perhaps formed during HST, but were prevented from evolving fully due to detrital influx associated with prograding clinoforms.

5. Onshore–offshore comparison

The New Jersey Coastal Plain Drilling Project is the onshore drilling component of the mid-Atlantic sea level transect (Miller et al., 1998b). Both onshore projects had excellent core recovery, so comparison with Sites 1071 and 1072, which had fairly poor recovery, are especially useful. Sequence boundaries can be identified more confidently onshore due to availability of outcrops and, more importantly, due to greater development of stratal geometries that permit recognition of sequence boundaries. However, direct correlation of onshore sites with Sites 1071 and 1072 may be difficult, in view of distances involved (Fig. 1), although this is an ongoing topic of post-Leg research.

Leg 150X sites included Island Beach (total depth = 372.7 m), Atlantic City (442.6 m), and Cape May (457.2 m) (Miller, 1997). (Fig. 1) Bass River was the single site drilled by 174AX, to a total depth of 596.34 m (Miller et al., 1998b). Several sequences

Table 3
Selected samples from Leg 174A Site 1072A

Site	Hole	Core	Section	Cm	Color	Shape	Maturity	K (%)	Sorting	Size dist.	% Glauc.	Mbsf
					Sequence			Boundary		PP4(S)		141–155
1072	A	25R	1W	20–22	Dark green	Subrounded	Hi ev		Homogeneous	Muddy sand	5–10	141.3
1072	A	26R	1W	120–122	V dark green	Rounded	hi ev	~8.7 hi ev	Moderately sorted	Muddy sand	≥90	146.3
1072	A	26R	1W	133–135	Dark green	Subrounded	hi ev	(9 hi ev	Moderately sorted	Muddy sand	≥70	146.3
1072	A	27R	1W	20–23	Dark green	Subrounded hi ev	hi ev	~8.7 hi ev	Poorly sorted	Sand	≥90	150.9
1072	A	27R	1W	21–23	Dark green	Sub-rounded	ev-hi ev	7.75 ev	Poorly sorted	Sand	~100	150.9
1072	A	27R	1W	81–83	V dark green	Rounded	hi ev	~9 hi ev	Poorly sorted	Sand	≥90	150.9
1072	A	27R	1W	102–104	Dark green	Sub-r-rounded	ev-hi ev	(9 hi ev	Poorly sorted	Sand	~100	150.9
1072	A	30R	ccw	8.0–10	Dark green	Subrounded	Evolved?		Poorly sorted	Sandstone	~40	165.3
					Sequence			Boundary		PP5(S)		225–249
1072	A	46R	5W	99–101	Green-dk g	Subrounded	hi ev	7–8 ev		Muddy sand	5–10	250.7
1072	A	46R	6W	42–44	Dark green	Subrounded	Evolved	~6.7 ev	V. poor	Muddy sand	30–40 ?	252.2
1072	A	47R	1W	6.0–9	Dark green	Rounded	ev-hi ev	~8.ev-hi ev	V. poor	Silty sand	≤50	254.2
1072	A	47R	1W	39–41	Green to dk g	Sub-rounded to rounded	ev-hi ev	~7.9 ev	V. poor	Silty sand	30–50 ?	254.2
					Sequence			Boundary		M0.5(S)		278–308

Table 4
Selected samples from Leg 174A Site 1071C

Site	Hole	Core	Section	Cm	Color	Shape	Maturity	K (%)	sorting	Size dist.	% Glauc.	Mbsf
					Sequence			Boundary		PP4(S)		124–138
1071	C	10X	Ccw	10.0–12.0	Dark green	Sub-rounded	hi ev	7.75 ev	Bioturbated	Fine sand	99	134
					Sequence			Boundary		PP5(S)		156–172
1071	C	16X	2W	113–115	It to dk green	Sub-rounded	hi ev		Poor	Muddy sand	~30	173.3
1071	C	16X	3W	24–27	Dark green	Subrounded	ev-hi ev	⩾9 hi ev	Poor	Muddy sand	~40	174.8
1071	C	16X	ccw	15–18	Green	Subrounded	ev-hi ev	>9 hi ev	Poor	Muddy sand	~30	175.15
1071	C	18X	ccw	3.0–5	Green-dk g	Subangular	Evolved	>9 hi ev	Well-sorted	Gravel	<1	190.8
1071	C	19X	1W	56–58	Green	Rounded	hi ev	~6 sl ev-ev	Bioturbated	Silty and muddy sand	10–20	200.1
1071	C	20X	3W	117–119	Dark green	Subrounded	ev	8.8 hi ev	V. poor	Glauc is silt in clay	~40	212.5
1071	C	20X	4W	10.0–12	Dark green	Subrounded	hi ev	6.5 ev	V. poor	Silty sand	Almost all	214
					Sequence			Boundary		M0.5(S)		233–257

have been identified at all four locations (Miller et al., 1998b) and we have completed a preliminary comparison of glauconite on- and offshore occurrence.

5.1. Onshore glauconite and systems tract occurrence

Onshore, glauconite is found the Eocene in the Absecon Inlet, Shark River, and Manasquan Formations. The basal glauconite in the Manasquan Formation showed possible signs of transport (Miller, 1997).

In the Oligocena strata, glauconite is found in the O1 sequence. The glauconite present in the HST of the Oligocene appears to be reworked from the TST (Miller, 1997), consistent with the higher sedimentation rate expected nearshore during highstand and highstand shedding.

Glauconite is less prevalent during Miocene time, and is found, only in the oldest of the four sequences of the Kirkwood Formation. The sequences coarsen upward, indicating shallowing. The Kirkwood sequences consist of thin to absent basal sands, interpreted as TST, which are overlain by prodelta clayey silts (lower HST). These silts grade upsection to delta-front medium to coarse sands which are interpreted as upper HST (Miller, 1997). The lack of glauconite in the younger Kirkwood sequences is interpreted to indicate that increased sedimentation was interfering with glauconite formation. A decrease in magnitude of sea-level change by the Miocene (Haq et al., 1987) likely led to this increased sediment influx. In addition, clastic influx from onshore also increased in conjunction with Miocene climate change. Near the present-day shore, Miller et al. (1998a) found that Oligocene sequences are thin as a consequence of low siliciclastic and pelagic input, while Miocene sequences are thicker, due to increased sediment supply during that time, which caused termination of glauconitization.

5.2. Comparison with Leg 174A offshore sites

Termination of the glauconitization process evidently did not occur at Sites 1071, 1072, and 1073 until Plio–Pleistocene time, perhaps because those locations remained far enough from the shoreline to avoid heavy influxes of sediment, as suggested by the very thin pre-Plio–Pleistocene section (Austin et al., 1998). Drilling at Leg 174A slope Site 1073 revealed three lithologic units (Austin et al., 1998) (Fig. 3). Unit I (Pleistocene to Holocene(?)) is silty clay with minor intervals of sandy mud and rare sand beds and laminae. Glauconite occurs only toward the bottom of Unit I. Unit II (Pliocene–Oligocene) is silty clay with thin interbeds of silt and sand. Locally, it is foraminifer rich, glauconitic, diatomaceous, or composed of nannofossil chalk. Bioturbation is variable. Unit III (upper Eocene) is a thoroughly bioturbated, glauconite-bearing, clay-rich nanofossil chalk and nannofossil clay. The TST is the primary setting in which glauconite is found offshore.

Fig. 8 (from Miller, 1997) summarizes glauconite occurrence onshore over time. Glauconite occurs in similar settings both on- and offshore, most frequently in the TST. Owens and Sohl (1969) found onshore sequences to contain basal transgressive glauconite sands; this basal glauconite sand is equivalent to the condensed section of Loutit et al. (1988) and the upper TST of Posamentier et al. (1988) (Miller, 1997). The TSTs of the Eocene and Oligocene are, in general, composed of glauconite sand (Miller, 1997). Increasing relative sea-level moved the shoreline far enough inland that Leg 150X sites would presumably have received little sediment input, developing a condensed section. Slow sedimentation would have provided a conducive environment for glauconite formation. During Miocene time, Miller (1997) found only occasional glauconite in the TST. The magnitude of eustatic sea-level highs during the Miocene was not as great as during Eocene–Oligocene times (e.g. Haq et al., 1987). Therefore heavier sedimentation would have overwhelmed glauconitization during the Miocene closer to the shoreline.

6. Discussion

It is important to note that Sites 903 and 1073 are located on the upper continental slope, so models of shelfal sequence geometry (e.g. Fig. 2) are not directly applicable. At Sites 903 and 1073, sequence boundaries presumably represent correlative conformities because present-day water depths are greater than maximum inferred eustatic change (e.g. Haq et al., 1987). These locations were presumably never subaerially exposed. It is therefore more difficult to trace individual boundaries due to a lack of reflector truncation, and coalescence of reflectors (Loutit et

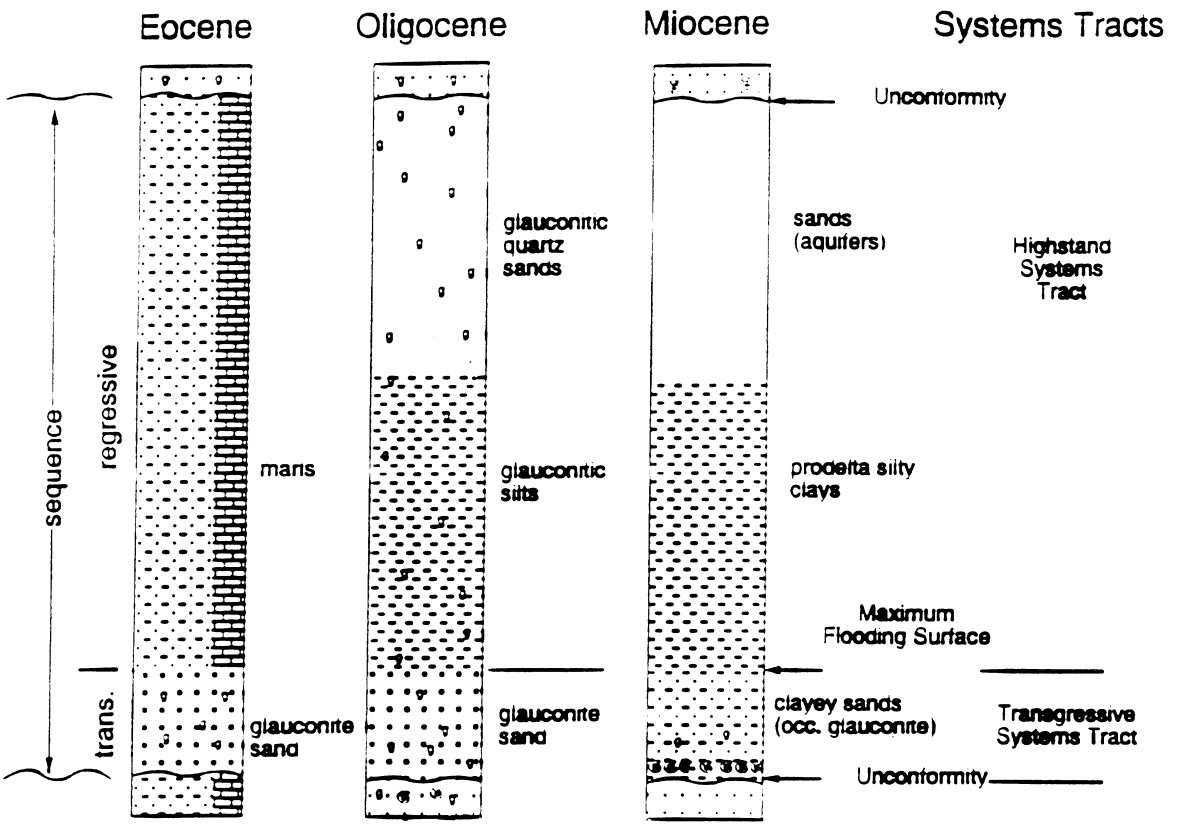

Fig. 8. Model for onshore occurrence of glauconite in a system-tract framework through time. Posamentier et al. (1988) systems tracts are shown on the right. Glauconite in Oligocene HST is reworked, trans. = transgressive, occ. = occasional. (From Miller, 1997).

al., 1988). The additional fact that Site 1073 is situated between two canyons (Fig. 1) may have resulted in significant sediment bypass, even during lowstand and early transgression, allowing it to remain sediment-free and thus glauconite could from during these intervals.

Based on the available seismic, γ-ray, lithologic, mineralogic, and sequence-stratigraphic evidence, the glauconites at Sites 903 and 1073 are interpreted to have formed during lowstand and transgression. G_{518} at Site 1073 is interpreted to have formed during the LST immediately above a sequence boundary (Fig. 7). G_{549} and G_{624} are interpreted to have formed in situ as part of distal condensed sections during transgression (Fig. 2). Glauconite may have begun formation in the HST, but evolution was prevented by the level of sediment input.

Despite broadly similar locations on the upper slope, Sites 903 and 1073 have different sedimentation histories. The 56 km distance and the presence of intervening canyons (Fig. 1) between the sites prevented a single sediment source from affecting both at the same time. Site 903 experienced sedimentation in the Miocene that filled a significant portion of the accommodation space (Fig. 6). Unlike the onshore sites, however, glauconitization continued at Site 903 throughout the Miocene. Site 1073 had significantly less sedimentation in the Miocene, glauconitization continued, and accommodation space was not appreciably filled until the Pleistocene. This time discrepancy prevents exact correlation between the glauconite deposits at the two sites.

We infer that glauconites at Sites 1071 and 1072 predominantly formed during TST, based on potassium content and maturity of the glauconites. Deposition was still minimal at these Sites during

early transgression, so there would have been a long enough time span for evolved to highly evolved glauconite to be created.

These results are in closer agreement with the geometry proposed by Austin et al. (1998) and Christie-Blick (1998) than with the traditional Exxon model predictions (e.g. Posamentier et al., 1988). The lack of accommodation space alters the sedimentation patterns in ways that are not accounted for in the Exxon model. For example, the LST is much thinner than expected, and may not even be present; the TST is deposited mainly on the shelf, filling accommodation space and leaving little room for a later HST. Therefore, the HST on the shelf is minimal due to a lack of accommodation space left by a thick TST, farther out in the basin the HST is expressed as prograding clinoforms (Fig. 2; Austin et al., 1998).

Onshore, glauconite is found in the TST during the Eocene and Oligocene and occasionally during the Miocene. Glauconite in the HST during the Oligocene appears to be recycled from the TST (Miller, 1997). We infer that the termination of glauconitization did not occur offshore until Plio–Pleistocene time because sea-level had remained high enough that significant sedimentation did not interface with the process. This is in contrast to the onshore locations that ceased glauconitization in the Miocene due to decreasing magnitude of eustatic sea-level change and therefore greater sedimentation and sediment flux although the rate of sedimentation is of course not solely controlled by sea level.

7. Conclusions

To summarize the main results of this study, the high potassium content and very mature glauconite formed during the early TST as part of the condensed section both on the shelf and onshore. Site 1073 possibly experienced more or less continuous formation of glauconite until the Plio–Pleistocene due to its location on the slope. Onshore, glauconitization ceased in the Miocene, yet continued until the Plio–Pleistocene on the outer shelf and upper slope. Overall, there is some predictability for glauconite occurrence is a systems-tract setting, within the context of local conditions. In this case, glauconite mainly formed in the TST, yet on a higher subsidence margin, or one with more sediment influx, the formation of glauconite would likely occur in a different time frame. Specifically, a higher rate of subsidence would allow aggradation over a longer time interval, keeping sediment input to a minimum on the outer shelf and upper slope. As a consequence, glauconite deposition could continue during the HST. Thus, higher subsidence rate margins would be expected to show a wider range of sequence-stratigraphic modes of glauconite occurrence (Table 1).

Implications of this study include the need for an integrated analysis and detailed study of glauconite occurrence along with seismic records, sedimentologic logs, and γ-ray and other physical data. We have shown there is no single sequence-stratigraphic setting for glauconite. Continued research, for example correlating sequence boundaries from 174A to onshore using recent R.V. Hatteras seismic data (Monteverde et al., 2000), may narrow the possibilities.

Acknowledgements

Funding for this project was provided by a JOI/USSSP grant to Whiting for Leg 174A post-cruise research. Greg Mountain (Lamont-Doherty Earth Observatory) provided migrated seismic data and a preliminary interpretation, James Hinthorne (Central Washington University) assisted with the XRD analysis, and Charles Knowles assisted with the SEM at the University of Idaho. XRD equipment acquisition at Central Washington University was partially supported by NSF grant 96-51022 (to J. Hinthorne). Reviews by P. Fullagar, G. Baum, M. Malone, S. Hesselbo and J. Austin greatly improved the quality of the manuscript.

References

am Ende, B., 1995. Evolution, environment, and isotope systematics of a glauconite deposit on the modern sea floor along the southeastern United States continental margin. PhD dissertation, University of North Carolina at Chapel Hill, 324pp.

Amorosi, A., 1995. Glaucony and sequence stratigraphy: a conceptual framework of distribution in siliciclastic sequences. Journal of Sedimentary Research B 65 (4), 419–425.

Austin, J.A., Jr., Christie-Blick, N., Malone, M., Berne, S., Borre, M.K., Claypool, G., Damuth, J., Delius, H., Dickens, G.,

Flemings, P., Fulthorpe, C., Hesselbo, S., Horton, T.E., III, Hoyanagi, K., Katz, M., Krawinkel, H., McCarthy, F., McHugh, C., Major, C., Mountain, G., Oda, H., Olson, H., Pirmez, C., Savrda, C., Smart, W.C., Sohl, L., Vanderaveroet, P., Wei, W., Whiting, B., 1998. Ocean Drilling Program Leg 174A Initial Report Continuing the New Jersey Mid-Atlantic Sea-level Transect. Ocean Drilling Program, Texas A&M University.

Baum, G.R., Vail, P.R., 1988. Sequence stratigraphic concepts applied to Paleogene outcrops, Gulf and Atlantic basins. In: Wilgus, C.K., Hastings, B.S., Kendall, C.G.S.C. (Eds.), Sea-level Changes: An Integrated Approach: SEPM Special Publication 42, Tulsa, OK, pp. 309–327.

Christie-Blick, N., 1990. Onlap, offlap, and the origin of unconformity-bounded depositional sequences. Marine Geology 97, 35–56.

Christie-Blick, N., Austin, J.A., Jr., ODP Leg 174A Shipboard Scientific Party, 1998. Unexpected facies architecture in sequences of late Miocene to Pleistocene age at the New Jersey outer continental shelf. Abstracts with Programs, Geological Society of America, Boulder, CO, pp. 266–267.

Greenlee, S.M., Schroeder, F.W., Vail, P.R., 1988. Seismic stratigraphic and geohistory analysis of Tertiary strata from the continental shelf off New Jersey; Calculation of eustatic fluctuations from stratigraphic data. In: Sheridan, R.E., Grow, J.A. (Eds.), The Atlantic Continental Margin, US, The Geology of North America I-2.: Geological Society of America, I-2, Geological Society of America, Boulder, CO, pp.437–444.

Greenlee, S.M., Devlin, W.J., Miller, K.G., Mountain, G.S., Flemings, P.B., 1992. Integrated sequence stratigraphy of Neogene deposits, New Jersey continental shelf and slope: Comparison with the Exxon model. Geological Society of America Bulletin 104, 1403–1411.

Haq, B.U., Hardenbol, J., Vail, P.R., 1987. Chronology of fluctuating sea-levels since the Triassic. Science 235, 1156–1167.

Hynes, A., 1990. Two-state rifting of Pangea by two different mechanisms. Geology 18, 323–326.

Loutit, T.S., Hardenbol, J., Vail, P.R., Baum, G.R., 1988. Condensed sections: the key to age determination and correlation of continental margin sequences. In: Wilgus, C.K., Hastings, B.S., Kendall, C.G.S.C. (Eds.), Sea-level Changes: An Integrated Approach: SEPM Special Publication 42, Tulsa, OK, pp. 183–213.

Manheim, F.T., 1967. Evidence for submarine discharge of water on the Atlantic continental slope of the southern United States, and suggestions for further research. Transactions of the New York Academy of Science: Series 2 v. 29, 839–853.

McCracken, S.R., Compton, J., Hicks, K., 1994. Sequence-stratigraphic significance of glaucony-rich lithofacies at Site 903. In: Mountain, G.S., Miller, K.G., Blum, P., Poag, C.W., Twichell, D.C. (Eds.), Proceedings of the Ocean Drilling Program Leg 150 Scientific Results, Ocean Drilling Program, Texas A&M University, pp. 171–187.

Miller, K.G., 1997. Coastal plain drilling and the New Jersey Sea-level transect. In: Miller, K.G., Snyder, S.W. (Eds.), Proceedings of the Ocean Drilling Program Leg 150X Scientific Results, Ocean Drilling Program, Texas A&M University, pp. 3–12.

Miller, K.G., Mountain, G.S., 1996. The Let 150 Shipboard party, and members of the New Jersey Coastal Plain Drilling Project, Drilling and dating New Jersey Oligocene–Miocene sequences: ice volumes, global sea-level, and Exxon records. Science 271, 1092–1095.

Miller, K.G., Mountain, G.S., Borwning, J.V., Kominz, M., Sugarman, P.J., Christie-Blick, N., Katz, M.E., Wright, J.D., 1998. Cenozoic global sea-level, sequences, and the New Jersey transect: result from coastal plain and continental slope drilling. Reviews of Geophysics 36 (4), 569–601.

Miller, K.G., Sugarman, P.J., Browning, J.V., Olsson, R.K., Pekar, S.F., Reilly, T.J., Cramer, B.S., Aubry, M-P., Lawrence, R.P., Curran, J., Stewart, M., Metzger, J.M., Uptegrove, J., Bukry, D., Burckle, L.H., Wright, J.D., Feigenson, M.D., Brenner, G.J., Dalton, R.F., 1998. In: Proceedings of the Ocean Drilling Program Leg 174AX Bass River Site. Ocean Drilling Program, Texas A&M University.

Monteverde, D.H., Miller, K.G., Mountain, G.S., this volume. Correlation of offshore seismic profiles with onshore New Jersey Miocene sediments, Sedimentary Geology (this volume), in review.

Mountain, G.S., Miller, K.G., Blum, P., Alm, P., Aubry, M., Burckle, L.H., Christensen, B.A., Compton, J., Damuth, J.E., Deconinck, J., de Verteuil, L., Fulthorpe, C.S., Gartner, S., Guerin, G., Hesselbo, S.P., Hoppie, B., Katz, M.E., Kotake, N., Lorenzo, J.M., McCracken, S., McHugh, C.M., Quayle, W.C., Saito, Y., Snyder, S.W., ten Kate, W.G., Urbat, M., Van Fossen, M.C., Vecsei, A., 1994. Volume 150 Initial Reports New Jersey Continental Slope and Rise. Ocean Drilling Program, Texas A&M University.

Odin, G.S., Matter, A., 1981. De glauconiarium origine. Sedimentology 28, 611–641.

Odin, G.S., Fullagar, P.D., 1988. Geological significance of the glaucony facies. In: Odin, G.S. (Ed.). Green Marine Clays Oolitic Ironstone Facies, Verdine Facies, Glaucony Facies and Celadonite-bearing Facies—a Comparative Study, Elsevier, Amsterdam, pp. 295–332.

Owens, J.P., Miller, K.G., Sugarman, P.J., 1997. Lithostratigraphy and paleoenvironments of the Island Beach borehole, New Jersey Coastal Plain Drilling Project. In: Miller, K.G., Snyder, S.W. (Eds.), Proceedings of the Ocean Drilling Program, Leg 150X Scientific Results. Ocean Drilling Program, Texas A&M University, pp. 15–24.

Owens, J.P., Sohl, N.F., 1969. Shelf and delatic paleoenvironments in the Cretaceous–Tertiary formations of the New Jersey coastal plain. In: Subitsky, S. (Ed.). Geology of Selected Areas in New Jersey and Eastern Pennsylvania and Guidebook of Excursions, Rutgers University Press, New Brunswick, NJ, pp. 235–278.

Posamentier, H.W., Jervey, M.T., Vail, P.R., 1988. Eustatic controls on clastic deposition I: Conceptual framework. In: Wilgus, C.K., Hastings, B.S., Kendall, C.G.S.C. (Eds.). Sea-level Changes: an Integrated Approach, Special Publication 42SEPM, Tulsa, OK, pp. 109–124.

Steckler, M.S., Watts, A.B., Thorne, J.A., 1988. Subsidence and basin modeling at the U.S. Atlantic passive margin. In: Sheridan, R.E., Grow, J.A. (Eds.). The Atlantic continental margin, US, The Geology of North America I-2, Geological Society of America, Denver, CO, pp. 399–416.